Increase in the Photoreactivity of Uracil Derivatives by Doubling Thionation

Marvin Pollum,[†] Steffen Jockusch,[‡] and Carlos E. Crespo-Hernández*[,†]

[†] Department of Chemistry and Center for Chemical Dynamics, Case Western Reserve University, Cleveland, Ohio 44106, United States; email: carlos.crespo@case.edu

[‡] Department of Chemistry, Columbia University, New York 10027, United States

Electronic Supporting Information

Photoproduct formation between the thiouracil derivatives and 5'-AMP

The changes observed in Figure 5 were further confirmed to be due to a light-induced reaction between the thiouracil derivative and 5'-AMP by irradiating solutions at 365 nm that contained only the thiouracil derivative. These solutions exhibited a much slower decrease in the UVA absorption band of the thiouracil derivative and the spectra displayed different isosbestic points from those reported in the main text for the thiouracil-5'-AMP mixtures. These isosbestic points occurred at 207, 292, and 354 nm for 4tUra and at 222, 243, and 393 nm for 2,4dtUra. These observations suggest that different photoproducts are formed when 5'-AMP is present in solution. Notably, solutions of the thiobase-5'-AMP mixtures, analogous to those used in Figure 5, showed no signs of reactivity when stored in the dark for three and a half days of monitoring. Hence, as discussed in the main text and reported previously,[1] steady-state absorption spectroscopy can be used to monitor the photoreaction between the 4tUra or 2,4dtUra and 5'-AMP by following the decay of the UVA absorption band of the thiouracil derivative. However, obtaining information about the photoproducts that are formed and the rate of their formation is less straightforward from these steady-state absorption experiments. Figure 5 shows that in both thiouracil-5'-AMP mixtures the photoproduct(s) being formed only absorbs in the UVB (280 to 315 nm) and UVC (100 to 280 nm) regions of the spectrum—regions where the thiouracil derivatives and 5'-AMP also absorb strongly. Therefore, in the UVB and UVC regions, the

decrease in absorbance of the reactants (thiouracil and 5'-AMP) is convoluted with the increase in absorbance of the photoproduct(s).

Under the experimental conditions used in our work (a 1:5 thiobase:5'-AMP molar ratio and N_2-saturated solutions), a 1-to-1 photoreaction between the photoexcited thiouracil derivatives and 5'-AMP can be expected, which leads to the formation of only one major photoproduct. This is supported by the photoreaction results obtained by Saintomé et. al. using equimolar mixtures of 4-thiothymidine and adenosine.[2] Hence, one way to deconvolute the absorption spectra of the reactants from that of the major photoproduct is by determining the difference spectrum at each time point throughout the photoreaction.

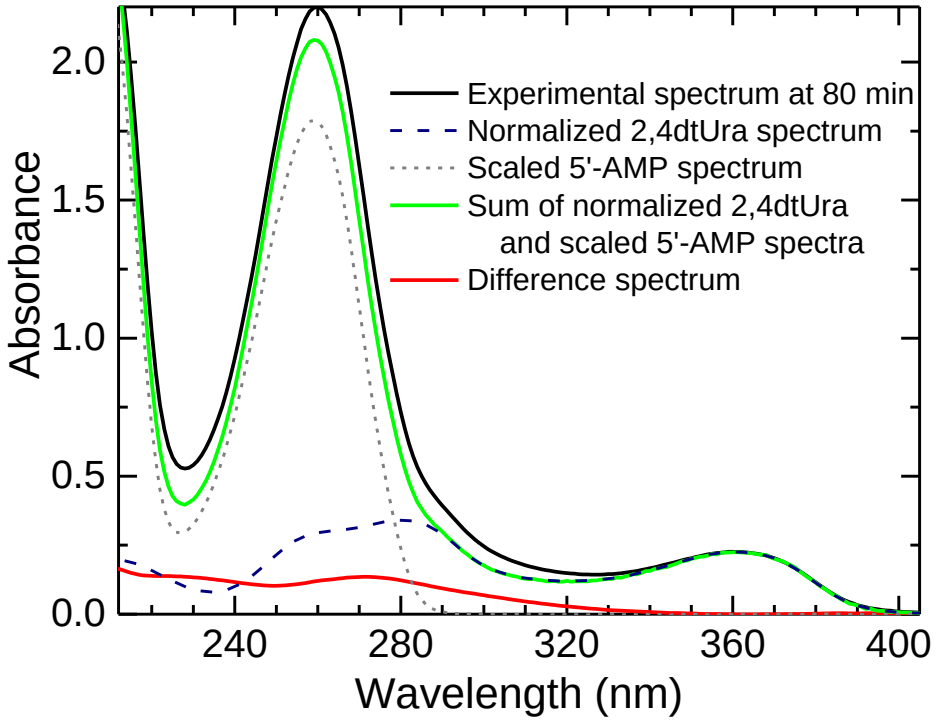

Figure S1. Representative plot depicting the method used to obtain the difference spectrum at each time point during the photoreaction experiments. The individual thiouracil (navy) and 5'-AMP (gray) spectra use for this were collected in pH 7.4 aqueous phosphate buffer at similar concentrations to the thiouracil-5'-AMP mixture being investigated. The contribution of the thiouracil absorbance to the experimental spectrum at each time point was determined by normalizing the thiouracil absorption spectrum to the experimental spectrum at the UVA absorption maximum. Then, assuming a 1-to-1 thiouracil-5'-AMP photoreaction, the concentration and corresponding absorption spectrum of 5'-AMP remaining in solution could be determined. The difference between the summed thiouracil-5'-AMP spectrum (green) and the experimentally observed spectrum at the corresponding time point (black) therefore produces the absorption spectrum of the photoproduct (i.e. the difference spectrum, red).

Figure S1 provides a representative example of how the difference spectrum is determined at each interval of irradiation shown in Figures 5 and 6. Conveniently, the photoproduct absorption in the UVA region is negligible, which enables the concentration of thiouracil derivative remaining in the solution to be determined at any given interval of irradiation. Using the normalized absorption spectrum and the molar absorptivity of the thiouracil derivative (Figure 1), the contribution of the absorption spectrum of the thiouracil derivative to the total absorbance of the mixture at different intervals of irradiation can be determined. Furthermore, the contribution of the absorbance of 5'-AMP to the total absorbance of the mixture can then be calculated with knowledge of its molar absorptivity (15,400 M^{-1} cm^{-1} at 259 nm),[3] since the decrease in concentration of 5'-AMP is equal to the decrease in concentration of the thiouracil derivative (assuming a 1-to-1 reaction). Then, a linear combination of the two calculated absorption spectra at a given interval of irradiation (i.e., the normalized spectrum of the thiouracil derivative and the scaled spectrum of 5'-AMP) can be subtracted from the corresponding absorption spectrum of the mixture to obtain a difference absorption spectrum. The difference absorption spectrum, shown in Figure S2, should correspond to the spectrum of the major photoproduct—the species that was not present in the solution before irradiation. The absorbance of the major photoproduct increases linearly with irradiation time (Figure S3), as might be expected for the relatively short extent of degradation used in this work (~6 to 20%, see Figures 5 and 6).

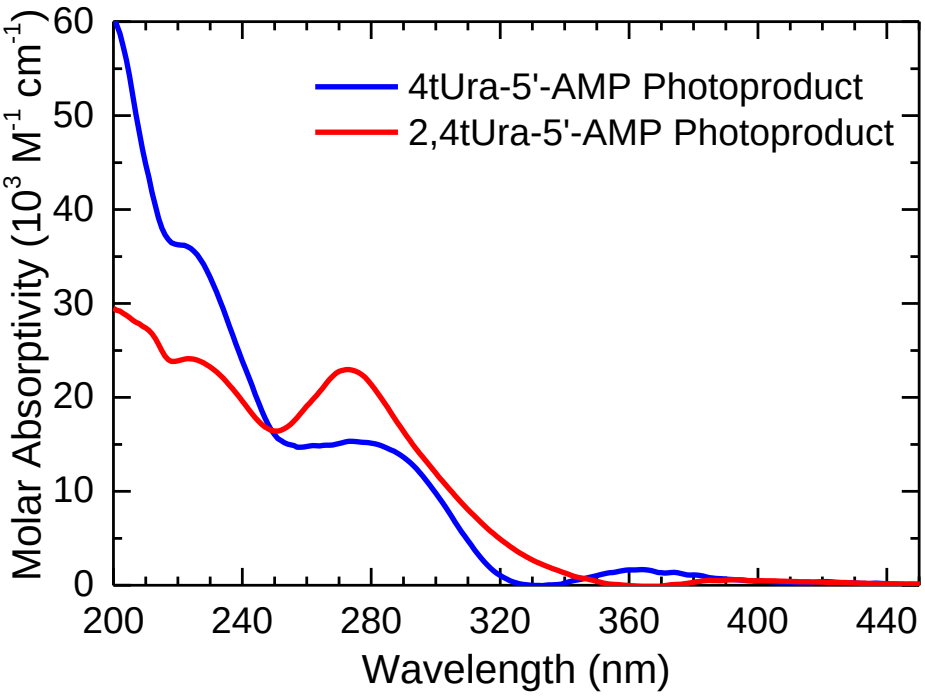

Figure S2. Effective molar absorptivity spectra for the primary photoproduct formed between 4tUra and 5'-AMP and between 2,4dtUra and 5'-AMP. The absorption spectra of these photoproducts was determined using the methodology describe in the supporting text and in Figure S1.

The molar absorptivity spectrum of the major photoproduct can also be estimated because its concentration at any given interval of irradiation should be equal to the change in concentration of thiouracil derivative (or 5'-AMP) at each irradiation time interval. Using this information, the photoproduct formation rate can be determined and should be equal to the photodegradation rate of thiouracil derivative (see Figure S3). Importantly, the molar absorptivity calculated for the product formed between 4tUra and 5'-AMP (12,780 M^{-1} cm^{-1} at 293 nm) is in good agreement with that measured for the chromatographically-purified major photoproduct of 4-thiothymidine and adenosine (13,840 M^{-1} cm^{-1} at 293 nm),[2] further supporting the methodology used in this work. As discussed in the next section, the similar photochemistry of these three reactions allows us to propose a mechanism for the formation of the major photoproduct between both thiouracil derivatives with 5'-AMP.

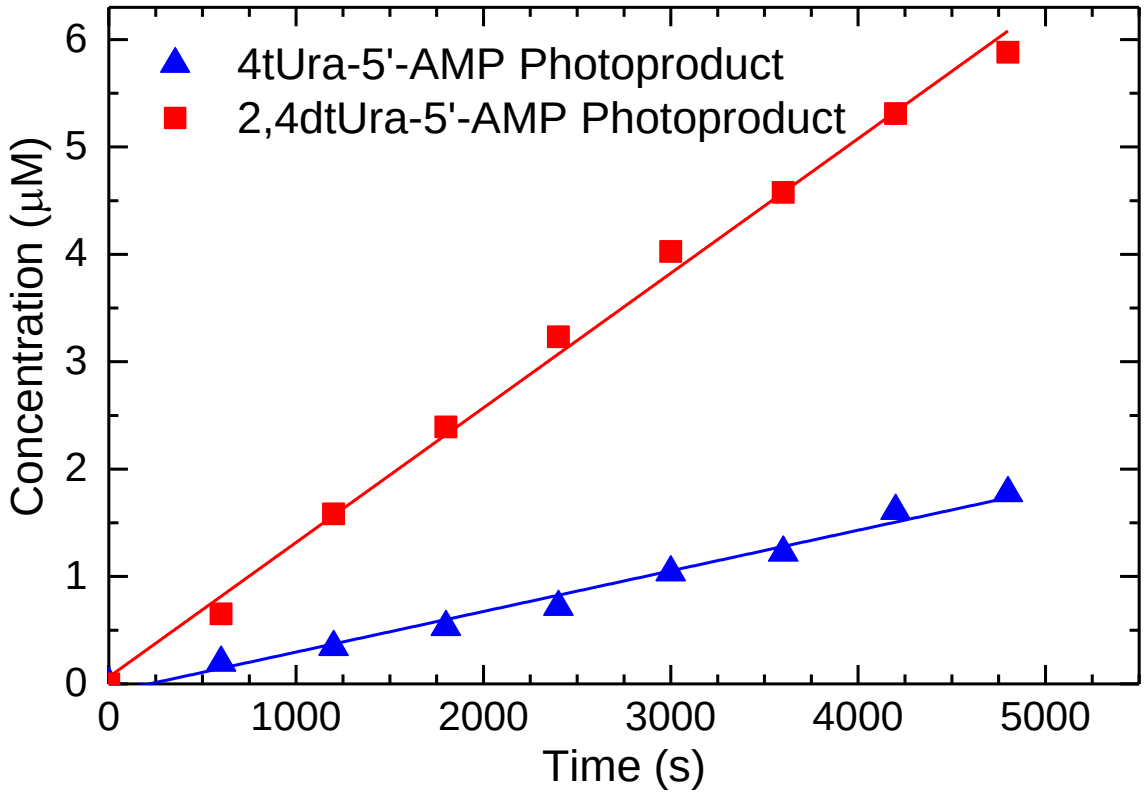

Figure S3. Change in concentration of the major photoproduct between the thiouracil compound and 5'-AMP as a function of the irradiation time at 365 nm. Photoproduct concentrations were determined using the estimated epsilon values at the 273 nm peak (Figure S2). Linear fitting of this data produced photoproduct formation rates equal to the UVA decay rates reported in the main text [$(0.39 \pm 0.04) \times 10^{-9}$ M/s for the 4tUra-5'-AMP mixture and $(1.2 \pm 0.2) \times 10^{-9}$ M/s for the 2,4dtUra-5'-AMP mixture], as can be expected for a 1-to-1 photoreaction leading to one major photoproduct.

It should be remarked that in addition to the major photoproduct, a minor, relatively insignificant photoproduct seems to be formed in the thiouracil-5'-AMP solutions irradiated in this work. Figure S2 shows a small absorption band that is redshifted from the lowest-energy absorption band of the parent thiouracil derivative. A similar absorption band is observed in the difference spectra of irradiated solutions of both thiouracil derivatives without 5'-AMP (data not shown). Hence, the minor redshifted absorption band is due to the formation of a photoproduct directly from the thiouracil derivative. This product is likely the (5-4) and/or (6-4) pyrimidine-pyrimidone photoproduct observed in irradiation experiments of 4tUra,[4-7] in the canonical pyrimidine bases,[8] and in 4-thiothymidine.[9]

Mechanism of photoproduct formation between the thiouracil derivatives and 5'-AMP

As described above, the absorption spectra of the photoproducts (Figure S2) support the idea that a single, major photoproduct is formed in the 4tUra-5'-AMP and 2,4dtUra-5'-AMP solutions used in this work upon irradiation at 365 nm and that the mechanism should be similar to that proposed for the photoreaction between 4-thiothymidine and adenosine.[2] Hence, we present a photoreaction mechanism in Scheme S1, which has been adapted from that reported in reference [2] to include the thiouracil derivatives used in this work. Briefly, Saintomé et. al.[2] showed that the C4-thione group of photoexcited 4-thiothymidine attacks the imidazole ring of the adenine chromophore across its N7=C8 double bond, undergoing a [2+2] cycloaddition that forms an unstable intermediate (**1**). The unstable heterocycle intermediate breaks at the C4 carbon-sulfur bond, leading to the transfer of the sulfur atom onto the C8 position of the adenine chromophore and the formation of a stable crosslink between the C4 carbon atom of the pyrimidine base and the N7 nitrogen atom of adenine chromophore (**2**). The imidazole ring of the adenine chromophore then undergoes ring opening at the N7 position and the loss of the labile thiol group through hydrolysis, thus forming the final cross linked photoproduct (**3**). The photoproduct shown in Scheme S1 for the reaction of 4-thiothymidine with adenosine was characterized using NMR, mass spectrometry, absorption spectroscopy, and X-ray crystallography, and shown to be the major product.[2]

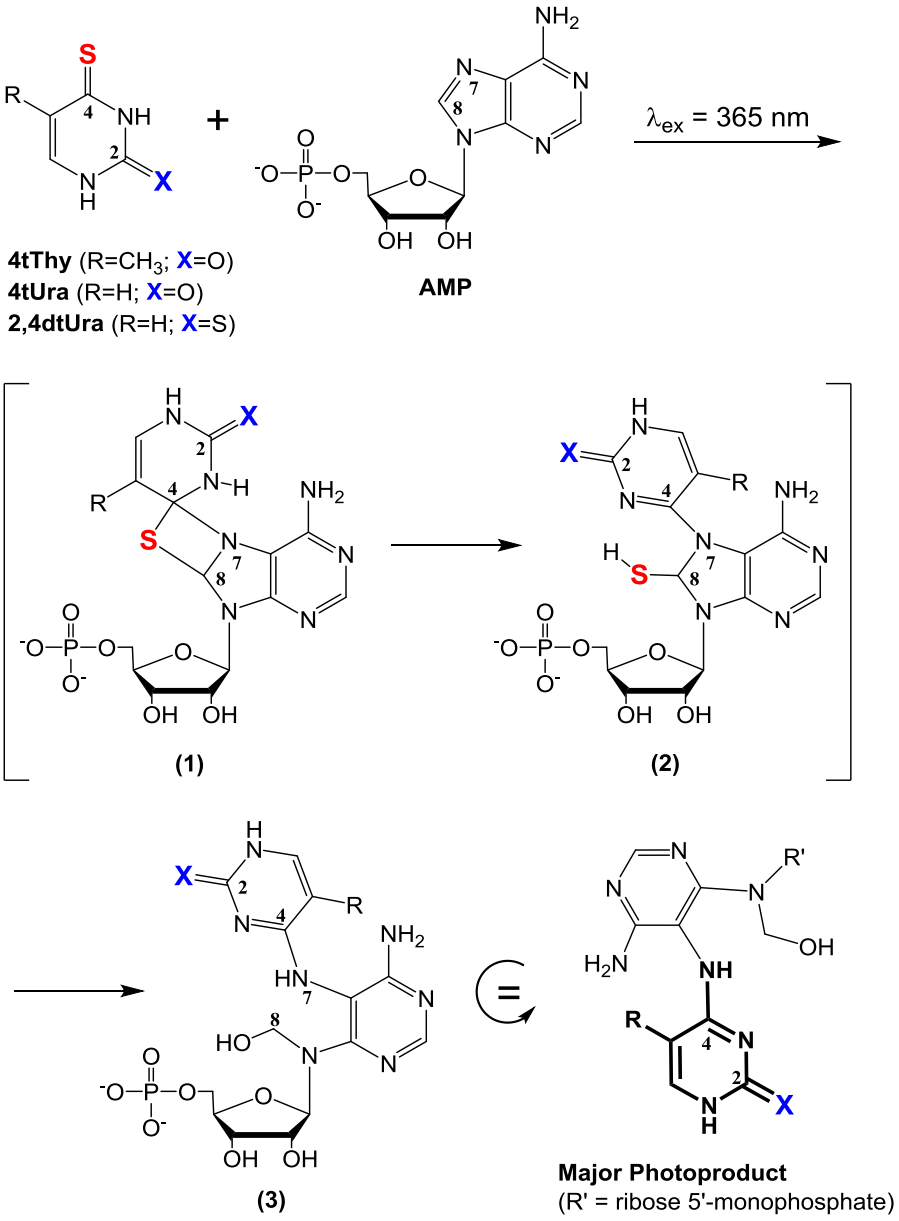

Scheme S1. Proposed photoproduct formation mechanism for the reaction between the thiouracil compounds (4tUra and 2,4dtUra) with 5'-AMP. This scheme was adapted from ref. [2]. 4-thiothymine (4tThy) instead of 4-thiothymidine is shown here for simplicity. The structure of the photoproduct highlights (in bold) its similarity to the cytosine and 2-thiocytosine chromophores that are expected to be formed depending on which thiouracil compound is photoreacting with 5'-AMP.

Highlighted in bold in Scheme S1 is the primary chromophore of the major photoproduct between 4-thiothymidine and adenosine, which has the same structure as that of 5-methylcytosine. In fact, the absorption spectrum of the major photoproduct was shown to be

similar to that of 5-methylcytosine, but with a slightly redshifted absorption band and greater molar absorptivity.[2, 10] If the photoreaction mechanism described in Scheme S1 also applies to the major photoproduct formed between the thiouracil derivatives and 5'-AMP, one would expect that its absorption spectrum should be similar to that of cytosine or 2-thiocytosine for 4tUra and 2,4dtUra, respectively, but with a slightly redshifted absorption band and a greater molar absorptivity. A comparison of the photoproduct spectra shown in Figure S2 to those of cytosine and 2-thiocytosine shown in Figure S4 supports this hypothesis. These semi-quantitative observations are summarized in Table S1 and lend further support to the idea that the photoreaction mechanism between the thiouracil derivatives and 5'-AMP is analogous to that reported between 4-thiothymidine and adenosine.[2] However, a rigorous validation of this mechanism awaits chromatographic separation and analytical characterization of these photoproducts.

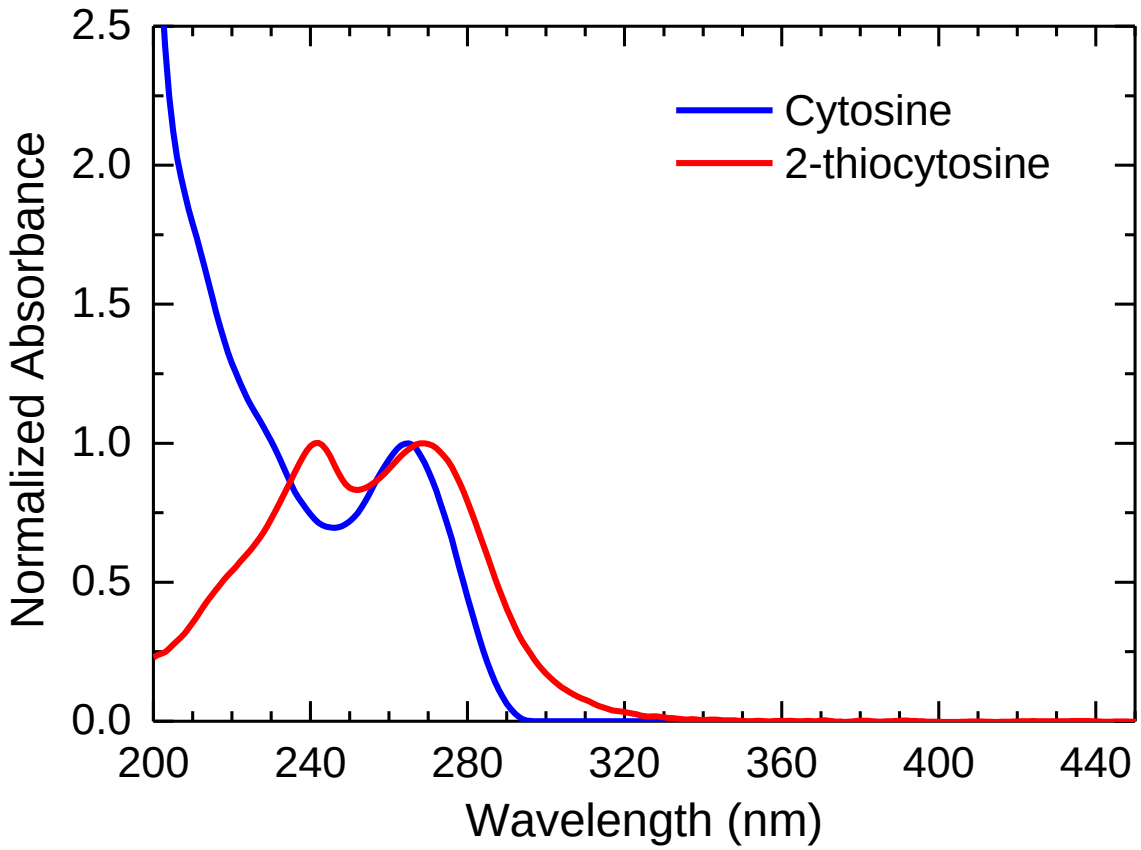

Figure S4. Absorption spectra of cytosine and 2-thiocytosine in aqueous buffer solutions normalized at their lowest-energy absorption band. These spectra should be compared with the absorption spectra of the photoproducts shown in Figure S2 and support the proposed photoreaction mechanism (Scheme S1).

Table S1. Comparison of the absorption properties of the primary photoproduct with those of the structurally-similar cytosine derivatives

Reactants	Primary photoproduct absorption properties		Cytosine derivative	Cytosine derivative absorption properties	
	$\lambda_{max.}$ (nm)	ε_{λ} (M^{-1} cm^{-1})		$\lambda_{max.}$ (nm)	ε_{λ} (M^{-1} cm^{-1})
4tThd and Ado	293	13,840	5-methylcytosine	274	6,260
4tUra and 5'-AMP	273	15,300	Cytosine	266	6,200
2,4dtUra and 5'-AMP	273	23,000	2-thiocytosine	270	18,200

Determining the enhanced near-visible absorption and photoactive tissue depth of 2,4dtUra

From an application-based perspective, it is important to quantify the enhanced ability of 2,4dtUra to absorb longer wavelengths of radiation than 4tUra. The use of longer excitation wavelengths reduces the direct absorption of radiation by native biomolecules and reduces the attenuation of radiation intensity from scattering as it travels deeper through tissue to reach the desired treatment area. Hence, the use of longer wavelengths of radiation can greatly enhance the efficacy of a photosensitizer. This is particularly true when moving from the UV to the visible region of the spectrum.[11-13]

In this work, we have quantified the near-visible absorption of 2,4dtUra and 4tUra by integrating their molar absorptivity spectra (Figure 1) in the region from 380 to 400 nm. This region of the spectrum is defined as "near-visible" herein because 380 nm is the shortest radiation wavelength that is visible to the human eye (violet).[14-16] However, other authors define the 400 nm as the beginning of the visible region of the spectrum.[17-19] The integration procedure gives the absolute area values of 1.5 and 41 for 4tUra and 2,4dtUra, respectively, corresponding to a 27.3-fold increase in the near-visible absorption cross-section.

The photosensitization enhancement provided by 2,4dtUra is further highlighted by looking at the experimental conditions used in the applications which currently employ 4tUra. The typical irradiation wavelength used in the photosensitization applications of 4tUra is 365 nm.[20-28] The molar absorptivity coefficient at this wavelength for 4tUra is 640 M^{-1} cm^{-1}. Therefore, we used the magnitude of the molar absorptivity coefficient of 4tUra at 365 nm as a threshold value (or cutoff criterion) to estimate the longest wavelength at which 2,4dtUra could be used as an effective photosensitizer (see Figure 7 in main text). Using this cutoff criterion, we estimated that 395 nm is the longest effective wavelength that can be used in the case of 2,4dtUra for

photosensitization applications. Figure 7 of the main text shows the wavelength-dependent penetration depth of light into colorless, bloodless tissue, as quantified by van Gemert et al.,[12, 13] which demonstrates that excitation at 395 nm can penetrate about 65 μm into tissue; that is 140% deeper than radiation at 365 nm can penetrate.

References to Electronic Supporting Information

1 A. Favre, Y. L. Dubreuil and J.-L. Fourrey, *New J. Chem.*, 1991, **15**, 593-599.
2 C. Saintomé, P. C. A. Favre, J.-L. Fourrey and C. Riche, *J. Am. Chem. Soc.*, 1996, **118**, 8142-8143.
3 D. L. Nelson and M. M. Cox, *Lehninger Principles of Biochemistry*, W. H. Freeman, 5th edn., 2008.
4 D. E. Bergstrom and N. J. Leonard, *Biochemistry*, 1972, **11**, 1-9.
5 C. Salet, R. V. Bensasson and A. Favre, *Photochem. Photobiol.*, 1983, **38**, 521-525.
6 S. J. Milder and D. S. Kliger, *J. Am. Chem. Soc.*, 1985, **107**, 7365-7373.
7 X. Zou, X. Dai, K. Liu, H. Zhao, D. Song and H. Su, *J. Phys. Chem. B*, 2014, **118**, 5864-5872.
8 W. J. Schreier, P. Gilch and W. Zinth, *Annu. Rev. Phys. Chem.*, 2015, **66**, 497-519.
9 C. Reichardt and C. E. Crespo-Hernández, *Chem. Comm.*, 2010, **46**, 5963-5965.
10 G. R. Wyatt, *Biochem. J.*, 1951, **48**, 581-584.
11 C. Kielbassa, L. Roza and B. Epe, *Carcinogenesis*, 1997, **18**, 811-816.
12 M. J. C. van Gemert and A. J. Welch, *IEEE Engineering in Medicine and Biology Magazine*, 1989, **89**, 10-13.
13 Q. Peng, A. Juzeniene, J. Chen, L. O. Svaasand, T. Warloe, K.-E. Giercksky and J. Moan, *Rep. Prog. Phys.*, 2008, **71**, 056701-056728.
14 T. J. Bruno and P. D. N. Svoronos, *CRC Handbook of Fundamental Spectroscopic Correlation Charts*, Taylor & Francis Group, Boca Raton, FL, 2005.
15 R. W. Waynant, ed., *Lasers in Medicine*, CRC Press, Boca Raton, FL, 2002.
16 W. G. K. Backhaus, J. S. Werner and R. Kliegl, eds., *Color vision: perspectives from different disciplines*, Walter de Gruyter & Co., Berlin, Germany, 1998.
17 P. Karran and N. Attard, *Nat. Rev. Cancer*, 2008, **8**, 24-36.
18 D. L. Reger, S. R. Goode and D. W. Ball, *Chemistry Principles and Practice*, Brooks/Cole, Belmont, CA, 3rd edn., 2009.
19 R. A. Serway, C. Vuille and J. S. Faughn, *College Physics*, Brooks/Cole, Belmont, CA, 8th edn., 2009.
20 G. Thomas and A. Favre, *Eur. J. Biochem.*, 1980, **113**, 67-74.
21 A. Favre, G. Moreno, M. O. Blondel, J. Kliber, F. Vinzens and C. Salet, *Biochem. Biophys. Res. Commun.*, 1986, **141**, 847-854.
22 A. Favre, G. Moreno, C. Salet and F. Vinzens, *Photochem. Photobiol.*, 1993, **58**, 689-694.
23 E. J. Sontheimer, *Mol. Biol. Rep.*, 1994, **20**, 35-44.
24 A. J. Newman, S. Teigelkamp and J. D. Beggs, *RNA*, 1995, **1**, 968-980.

25 M. Hafner, M. Landthaler, L. Burger, M. Khorshid, J. Hausser, P. Berninger, A. Rothballer, M. A. Jr., A.-C. Jungkamp, M. Munschauer, A. Ulrich, G. S. Wardle, S. Dewell, M. Zavolan and T. Tuschl, *Cell*, 2010, **141**, 129-141.
26 K. Kramer, T. Sachsenberg, B. M. Beckmann, S. Qamar, K.-L. Boon, M. W. Hentze, O. Kohlbacher and H. Urlaub, *Nat. Methods*, 2014, **11**, 1064-1074.
27 A. Favre, R. Bezerra, E. Hajnsdorf, Y. L. Dubreuil and A. Expert-Bezançon, *Eur. J. Biochem.*, 1986, **160**, 441-449.
28 R. Bezerra and A. Favre, *Biochem. Biophys. Res. Commun.*, 1990, **166**, 29-37.